MESOSPHERIC TEMPERATURE INVERSION LAYERS: RECENT OBSERVATIONS FROM UARS ISAMS AND MLS

Dong L. Wu

Jet Propulsion Laboratory, California Institute of Technology

4800 Oak Grove Drive, Pasadena, CA 91109, USA

To be submitted as an article in the book *'Recent Research Developments in Geophysical Research'*, published by Research Signpost

Abstract

This paper presents an observational study of the mesospheric temperature inversion layer with Upper Atmosphere Research Satellite (UARS) Improved Stratospheric and Mesospheric Sounder (ISAMS) and Microwave Limb Sounder (MLS). The satellite data show that the temperature inversion layer can be generated from deep penetration of planetary waves in the mesosphere. For the period of interest (5 December 1991-13 January 1992), planetary wave activity was strong and dominated by stationary wave1 at middle and high latitudes. Good correlation is observed between modulation of transient wave1 events and enhancement of the inversion layer at 65-80km altitudes. In addition, the strongest planetary wave occurred around 15 December 1991 and led to a warming in the stratosphere and cooling in the mesosphere but the following events did not. The wave amplitude evolution at planetary and gravity-wave scales exhibits a strong connection between perturbations at high and low altitudes where a downward progression is evident in the peak amplitudes in the upper stratosphere and mesosphere, indicating that the perturbations start first at a higher altitude. However, understanding the cause of the inversion layer and its relation to planetary and gravity wave activity requires further dedicated investigations.

1. Introduction

The mesospheric temperature inversion layer is a phenomenon that the temperature lapse rate reverses sign at ~60-85km altitudes from negative to positive. Such temperature inversion, sometimes as high as some tens of Kelvin over a layer of 5-10km, is often observed in the winter hemisphere at latitudes greater than ~40°. Ground-based observations of the temperature inversion are mostly provided by rocket and lidar techniques [1-4]. Satellite temperature observations generally have a poorer vertical resolution but are shown capable to detect such temperature inversion feature [5-7]. Unlike the sharp temperature inversion structures seen in high-resolution lidar measurements, satellite observations catch these inversions at similar altitudes but with much weaker amplitude [6]. One of the advantages with satellite observations is the wider view of the temperature inversion layer that allows to study the roles of planetary-scale oscillations not observed by ground-based observers.

The mechanism(s) causing the temperature inversion layer remains unclear at present although some hypotheses have been proposed. One of the mechanisms proposed is based upon gravity wave breaking [7, 8], which thinks the turbulent heating generated by the wave breaking may be enough to reverse the lapse rate in the mesosphere. In addition to the gravity wave influence, planetary-scale waves have been suggested to be able to modulate the inversion layer. Observations show that the inversion layer altitude varies with local time, which is thought perhaps due to interactions with solar atmospheric tides [9-11].

In this study we analyze the UARS (Upper Atmosphere Research Satellite) data to show further evidence of formation/modulation of the mesospheric temperature inversion layer by planetary waves. The study is focused on the early period of UARS mission (5 December 1991-13 January 1992) when both the Improved Stratospheric and Mesospheric Sounder (ISAMS) and

the Microwave Limb Sounder (MLS) instruments observed the Northern Hemisphere winter. The temperature, geopotential height, and radiance variance measurements are used together in the analysis, and good correlation is found between the temperature inversion layer and planetary wave activity in the mesosphere.

2. Data and Analysis

The ISAMS data used in this study are V12 L3AT temperature at ~16-80km altitudes (essentially same as V10) [12,13]. The estimated error for a single profile varies between 2-12K with larger error at higher altitudes. The vertical resolution increases with height varying from ~7km in the stratosphere to ~20km in the upper mesosphere. During the period of 5 December 1991-13 January 1992 ISAMS observations cover latitudes of 34°S-80°N and the local times on ascending and descending nodes are ~00:00 and 12:00, respectively.

The MLS on board UARS had the nearly same latitude coverage and sample distribution for the period of interest. A special research algorithm is used for the mesospheric temperature and geopotential height retrieval. The retrieval algorithm was initially developed and applied for the 2-day wave study [14], and has been improved recently by incorporating a more accurate model for the geomagnetic Zeeman effect calculation. Temperature and geopotential height measurements are produced for 20-90km altitudes where the estimated precision of a single profile is ~2-15K for temperature with the larger error at higher altitudes. The vertical resolution of MLS temperature varies from 6km in the stratosphere to ~10km in the upper mesosphere.

A direct comparison between MLS and ISAMS temperatures is made to highlight differences of these measurements. The results of the point-by-point comparison are summarized in Table 1. MLS has a generally positive bias against ISAMS at all altitudes, which brings MLS temperature closer to the rocket measurements in the stratosphere and lower mesosphere than ISAMS [12].

The mean bias oscillates somewhat in the upper mesosphere, showing smaller values at 0.02-0.05hPa and larger differences at 0.1-0.2hPa, which is a similar feature in the temperature differences between ISAMS and HALOE (Halogen Occultation Experiment, another UARS instrument that measures mesospheric temperature) [12]. As a result, the MLS-ISAMS differences in the upper mesosphere imply better agreement between MLS and HALOS temperatures at these altitudes.

The scaling difference (the correlation coefficient between MLS and ISAMS temperatures) reflects temperature sensitivity differences between the two instruments. As shown in Table 1, the ratio is nearly 1:1 at altitudes up to ~50km and decreases above that altitude. A minimum value is found near 64km, where MLS is known to have poor temperature sensitivity. The scaling difference can also be caused by the retrieving schemes/parameters used. For example, the reference atmosphere or linearization values can cause measurement biases if the retrieval is constrained to these values in poor sensitivity cases. Hence, for poor sensitivity situations, MLS retrieval is worse than ISAMS because it is constrained a single profile while ISAMS is constrained to a latitude-and-season-dependent reference (i.e., the COSPAR International Reference Atmosphere) [15].

A temperature inversion index, defined as the temperature difference between 77km and 67km, is used to characterize occurrence of the mesospheric temperature inversion. These altitudes are chosen because statistically the minimum temperature of the inversion layer occurs at ~65km for the Northern Hemispheric winter [2]. Hence, positive index values indicate good likelihood to observe the temperature inversion layer. Because of the poor vertical resolution of these satellite measurements, we can only detect thick temperature inversion layers and neglect

sharp structures such as ones observed by ground-based lidars. A noisier index was used in other early studies with the ISAMS data [2,6] and yielded a similar result for the inversion layer.

To investigate its relation to small-scale wave activity, we also compare the inversion layer variation with the time series of MLS radiance variance that is obtained directly from the saturated radiances using the technique described by Wu and Waters [16]. The radiance variances measure atmospheric temperature fluctuations of horizontal scales of ~100km at 8 altitude layers from 28 to 80km. The thickness of the altitude layer is ~10km except for the highest layer (featured by the center channel) which is ~15km. MLS radiance variances consist of the instrument noise and atmospheric temperature fluctuations of long (>10km) vertical and short (~100km) horizontal wavelengths. The instrument noise is constant and can be readily removed from the total radiance to yield a variance due to atmospheric temperature variations.

3. ISAMS and MLS Observations

Figure 1 show a temperature inversion event observed by ISAMS at ~55°N latitude on 8 January 1992. The inversion layer occurred at a number of places in this latitude band, for example, at longitudes of 210°, 280°, 55°, and 175°, where low temperatures are found at ~70km altitude and high temperatures are near ~80km. Most incidences have a scale of 30°-50° in longitude (or 2000-3000km at this latitude), part of which clearly belongs to the strong planetary wave that penetrates into the mesosphere. As shown in the temperature perturbation in Figure 1(a), the planetary wave is dominated by zonal wavenumber 1 in the stratosphere and lower mesosphere, and mixed with wavenumber 2 in the middle and upper mesosphere. Smaller-scale fragments in the middle and upper mesosphere, not obviously associated with the wave1 pattern, also contribute to the temperature inversion at some longitudes.

A similar picture is seen in MLS temperature on the same day (Figure 2), except that the temperature inversions occur in larger areas and greater amplitudes. The extended altitude coverage of MLS temperature provides a more complete picture of the inversion layers and planetary waves. The geopotential height measurement from MLS shows that the strong wave1 event reaches 70-75km with peak amplitude of ~1.5km at ~70km (Figure 3). The wave1 amplitude decays rapidly above 75km where other wave components (e.g., wave 2 and 3) start to emerge. The maximum geopotential height amplitude occurs where the temperature amplitude is minimal.

The wave1 event on 8 January 1992 provides strong evidence that planetary waves can produce and significantly influence the mesospheric temperature inversion layer. To explore this relation in further detail, we extend the analysis to the period of 5 December 1991-13 January 1992 by comparing evolution of the temperature inversion index defined in Section 2 and the amplitude of stationary planetary wave1.

Figure 4 shows the time series of ISAMS temperature inversion and wave1 amplitudes at 53-74km altitudes. As indicated in the top panel, the temperature inversion occurs mostly in a latitude belt between 45°N-70°N, which mimics the pattern of wave1 amplitude at the same latitudes. During the period of interest, there are two major wave1 events as revealed with the wave amplitudes at ~69km. These transient wave events are correlated well with the modulation of the temperature inversion index. Again, this correlation confirms the inversion layer and planetary wave connection found with the 8 January 1992 event where mesospheric planetary waves could be responsible for the broad occurrence of the temperature inversion layer.

The same comparison is made for the temperature inversion layer and wave1 amplitude observed by MLS [Figure 5]. The results are similar to that with ISAMS data. However,

differences are evident in the evolution of temperature inversion and wave1. The differences may indicate a shortcoming of the temperature inversion index used. Because of variability associated with the inversion layers and different vertical resolution with these measurements, temperature differences between 67km and 77km altitudes may not be optimal for both instruments to detect the phenomenon. For example, as shown in Figure 6, MLS temperature differences between 80km and 69km would match well to the ISAMS observations in Figure 4.

Figure 6 also shows an anti-correlated relation between the temperature inversion and wave1 geopotential height amplitude. Comparing the temperature inversion with the wave1 amplitude at 69km, one can see modulation between the enhanced inversion and depressed wave1 amplitudes of geopotential height. For example, the wave1 event around 20 December is correlated with a short pause of temperature inversion during this period. A similar relation appears for the event near 10 January. This anti-correlation is not very clearly exhibited when the 77-67km difference is used.

Evolution of the wave amplitudes at different altitudes reveals a downward progression of the wave1 events in Figure 6, which shows that the amplitude peaks at a later time at a lower altitude. Figure 7 shows the downward progression more clearly with the wave1 amplitude of MLS temperature at 55°N. In the upper stratosphere and mesosphere, the downward progression appears to be a common feature for most of the wave1 events. In the middle and lower stratosphere, however, the upward progression of the wave1 amplitude is noted in some cases. For examples, the wave1 enhancement around 15 December is first observed at altitudes below ~35km before a peak is found at higher altitudes. In the meantime, the zonal mean temperature in Figure 8 shows that the strong wave1 event also caused the stratospheric warming and mesospheric cooling around 18 December.

To investigate the gravity-wave influence on the inversion layer, we analyze MLS small-scale radiance variances and show a time series of the zonal mean variance for the period of interest. These variances measure the intensity of gravity-wave-scale activity with large vertical (>10km) and small (~100km) horizontal scales at 40-80km altitudes (Figure 9) [16, 17]. Because the vertical resolution of MLS saturated radiances is comparable to the scale of the temperature inversion layers, the distortions like the inversion layer could contribute significantly to the radiance variances. Also because the radiance variances represent for variability of short horizontal scales, any good correlation may suggest the inversion layer as a localized event. Figure 9 shows two variance enhancement events: one around 15-18 December and the other near 1 January, both of which are slightly ahead of temperature wave1 and inversion events seen in Figures 4-5 at similar altitudes. Correlation between the inversion layer and the channel 7 variance (that features 61km) is significant but not as good as one with planetary wave1, which suggests that large part of the inversion layer could be associated with small-scale perturbations. Once again, a slight downward progression is evident among the variance enhancements at different altitudes, for example, showing that the first event occurred slightly after 15 December at 38km (channel 3) and near/before 15 December above 60km (channels 7 and 8).

4. Discussions and Summary

We have shown with MLS and ISAMS temperature data that the temperature inversion layers might have been strongly associated with planetary wave structures in the mesosphere. The event on 8 January 1992 suggests that the inversion events seen by ground-based observers could also be a consequence of planetary wave penetration/breaking in the mesosphere. As a result, the temperature inversion layer can occur in large areas and last for days.

Many researchers have been focusing on the breaking high-frequency gravity waves as the cause of the inversion layers [e.g. 4,8]. Such wave breaking would produce turbulent heating within the layer and convective cooling above it. It has been shown that the coupling of gravity and planetary waves can effectively alter the mesospheric thermal structure over a large area and bear some characteristics of the large-scale waves [18,19]. Model simulations suggest a plausible tidal/gravity wave interaction for enhancing local dynamical cooling and turbulent heating such that the descending heating/cooling structure mimics the tidal variation. This coupling mechanism qualitatively interprets the downward phase progression and magnitude of the inversion layer peak in lidar observations [11]. The mechanism might also work for the coupling between gravity and stationary planetary waves, and as a result, the inversion layer would mimic the planetary wave distribution. One could further explain the planetary wave to inversion layer relation observed by ISAMS and MLS as a manifestation of such coupling mechanism.

Nevertheless, the inversion layer can be also formed from planetary wave penetration/breaking, as revealed by ISAMS and MLS observations on 8 January 1992. This study highlights such connection by showing the satellite observations over 5 December 1991-13 January 1992 period and bringing together other related atmospheric information. We noticed that the strong planetary wave1 around 15 December 1991 led to a stratospheric warming while no warmings were associated with two following transient wave events during the period of interest. The evolutions of planetary wave and small-scale variance amplitudes both show a downward progression of the peak amplitude in the upper stratosphere and mesosphere, indicating a strong connection between disturbances at upper and lower levels. However, the generation and evolution of the inversion layer and related processes remain unclear at present and further dedicated investigations are needed.

5. Acknowledgments

This work was performed at the Jet Propulsion Laboratory, California Institute of Technology, under contract with the National Aeronautics and Space Administration, and supported by the NASA New Investigator Program in Earth Sciences. The author thanks Thierry Leblanc for helpful discussions.

Figure Captions

Figure 1. ISAMS measurement at ~52°N on 8 January 1992: (a) temperature perturbation about the longitudinal mean, and (b) temperature. Only descending-orbit measurements are shown with longitude labeled in the bottom of each plot. The contour intervals are 10K in both plots. There was a strong planetary wave1 perturbation on this day that penetrates deeply into the mesosphere creating the temperature inversion layer at 65-80km altitudes. The connection to the mesospheric planetary wave suggests another mechanism (other than gravity wave breaking) that might be responsible for the formation of the inversion layer.

Figure 2. Same as in Figure 1 but for MLS temperature at 52.6°N latitude. MLS is able to observe temperature at altitudes above 80km allowing a more complete view of the planetary wave and inversion layer features.

Figure 3. MLS geopotential height perturbations on 8 January 1992 for the same orbital and latitudinal conditions as in Figure 2. MLS geopotential height is derived from tangent pressure measurements and tangent heights that are determined by an encoder for antenna pointing encoder and UARS attitude/orbit information. The data are valid from the top of each scan (normally ~90km) to ~30km where the pressure sensitivity diminishes. The precision of geopotential height measurement varies with altitude from ~0.05km at 30km to ~0.03km at 50km, and to 0.4km at 90km. Contour intervals are 0.4km.

Figure 4. Time series of ISAMS inversion index, defined as a temperature difference between 77km and 67km (top panel), and wave1 temperature amplitudes at 53-74km during 5 December 1991-13 January 1992. For each latitude bin, both ascending and descending data are used to produce daily mean temperature inversion and wave1 amplitude. Contour

intervals are 4K for wave1 and 2K for temperature inversion.

Figure 5. As in Figure 4 but for MLS temperature.

Figure 6. MLS inversion index from the temperature differences between 80km and 69km (top panel) and wave1 geopotential height amplitudes at 53-74km. Contour intervals are 0.4km for geopotential height and 2K for temperature inversion.

Figure 7. MLS wave1 temperature amplitude at 55°N, showing evolution of the wave amplitude with time and height. Downward progression of the wave amplitude is clearly seen in the upper stratosphere and mesosphere for each transient event. The contour interval is 4K.

Figure 8. MLS zonal mean temperature at 55°N, showing a stratospheric warming and mesospheric cooling around 18 December 1991. This warming/cooling is associated with the strong wave1 event that occurred at about the same time.

Figure 9. Small-scale radiance variances from MLS showing amplitude modulations associated with planetary wave events. The variances of different spectral channels correspond to the measurements at different altitudes. Since MLS channels are symmetric about the line center, each pair of symmetric channels feature the same altitude layer. Contour intervals are $0.02K^2$ for channels 3 (38km) and 4 (43km), and $0.04K^2$ for the others.

Table 1. MLS-ISAMS Temperature Differences

Pressure (hPa)	Approx. Height (KM)	MLS-ISAMS Diff.(K)	Scaling Ratio
0.01	80	7.6	0.78
0.02	75	1.8	0.75
0.05	69	0.1	0.66
0.10	64	6.9	0.52
0.22	59	3.5	0.66
0.46	53	1.3	0.73
1.00	48	7.2	0.92
2.15	43	5.4	0.99
4.64	37	5.4	0.98
10.0	32	5.0	1.01
21.5	27	3.8	0.88
46.4	21	2.7	0.76

References

1. Schmidlin, F. J., 1976, *Geophys. Res. Lett.*, 3, 173-176.

2. Hauchecorne, A., M. L. Chanin, and R. Wilson, 1987, *Geophys. Res. Lett.*, 14, 933-936.

3. Meriwether, J. W., et al., 1994, *J. Geophys. Res.*, 99, 16,973.

4. Whiteway, J. A., A. I. Carswell, and W. E. Ward, 1995, *Geophys. Res. Lett.*, 22, 1201.

5. Clancy, R. T., D. W. Rusch, and M. T. Callan, 1994, *J. Geophys. Res.*, 99, 19,001.

6. Leblanc, T., et al., 1995, *Geophys. Res. Lett.*, 22, 1485-1488.

7. Leblanc, T., and A. Hauchecorne, 1997, *J. Geophys. Res.*, 98, 20,369-20,384.

8. Hauchecorne, A., and A. Maillard, 1990, *Geophys. Res. Lett.*, 17, 2197-2200.

9. Dao, P. D., R. Farley, X. Tao, and C. S. Gardner, 1995, *Geophys. Res. Lett.*, 22, 2825.

10. States, R. J. and C. S. Gardner, 1998, *Geophys. Res. Lett.*, 25, 1483-1486.

11. Meriwether, J. W. et al., 1998, *Geophys. Res. Lett.*, 25, 1479.

12. Dudhia, A., and N. Livesey, 1996, *J. Geophys. Res.*, 101, 9795.

13. Livesey, N., 1995, Ph.D. Dissertation, University of Oxford, UK, pp. 238.

14. Wu, D. L., E.F. Fishbein, W.G. Read, and J.W. Waters, 1995, *J. Atmos. Sci.*, **53**, 728.

14. Barnett, J. J., and M. Corney, 1985, *MAP Handb.*, 16, 47.

16. Wu, D. L., and J.W. Waters, 1996, *Geophys. Res. Lett*, **23**, 3631-3634.

17. McLandress, C., M. J. Alexander, D. L. Wu, 1999, *J. Geophys. Res.*, in press.

18. Walterscheid, R. L., *J. Geophys. Res.*, 1981, **86**, 9698.

19. Liu, H.L., and M. E. Hagan, 1998, *Geophys. Res. Lett.*, **25**, 2941.

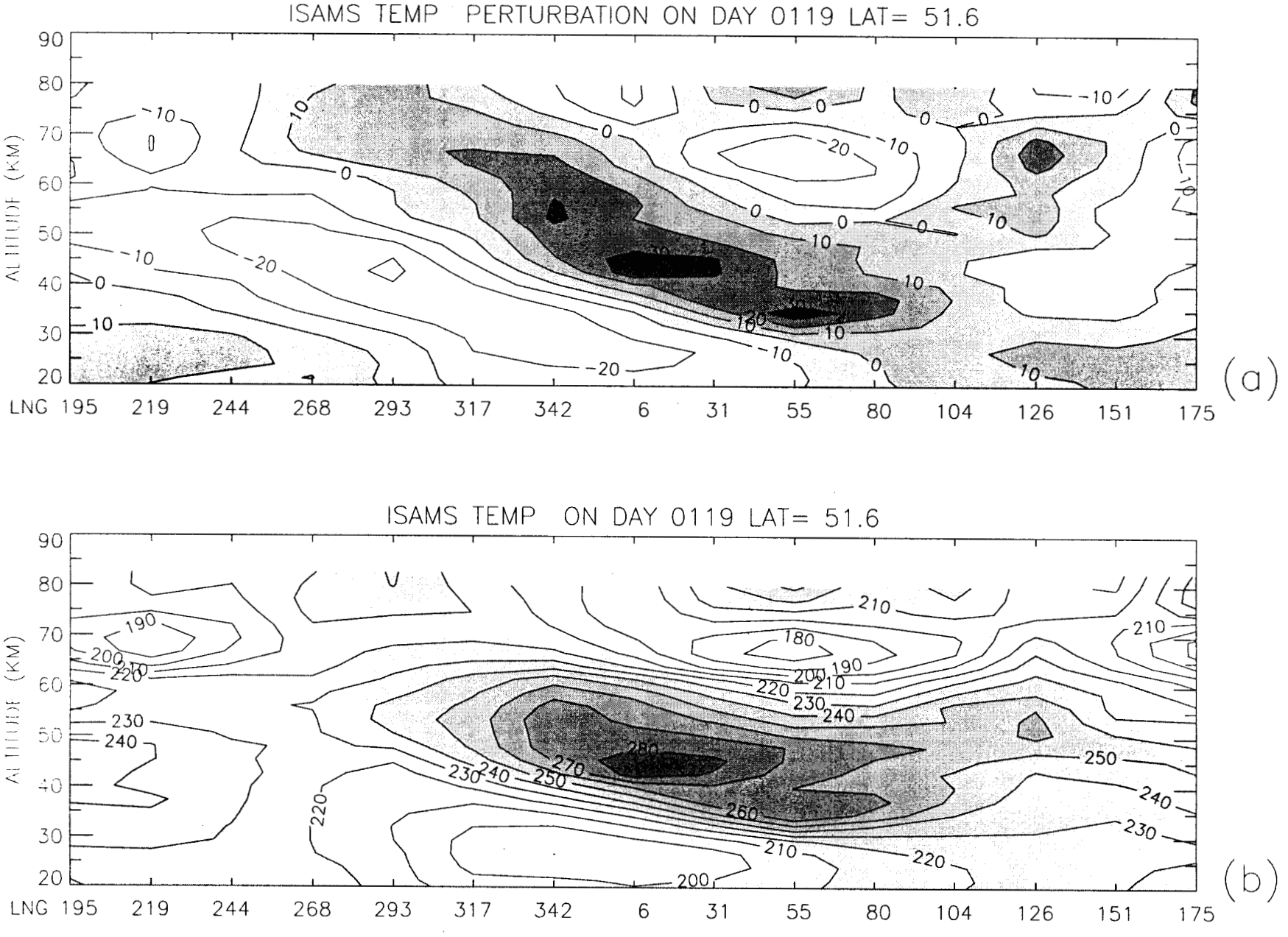
ISAMS TEMP PERTURBATION ON DAY 0119 LAT= 51.6
ALTITUDE (KM)
90
80
70
60
50
40
30
20
LNG 195 219 244 268 293 317 342 6 31 55 80 104 126 151 175
(a)
ISAMS TEMP ON DAY 0119 LAT= 51.6
ALTITUDE (KM)
LNG 195 219 244 268 293 317 342 6 31 55 80 104 126 151 175
(b)

Figure 1.

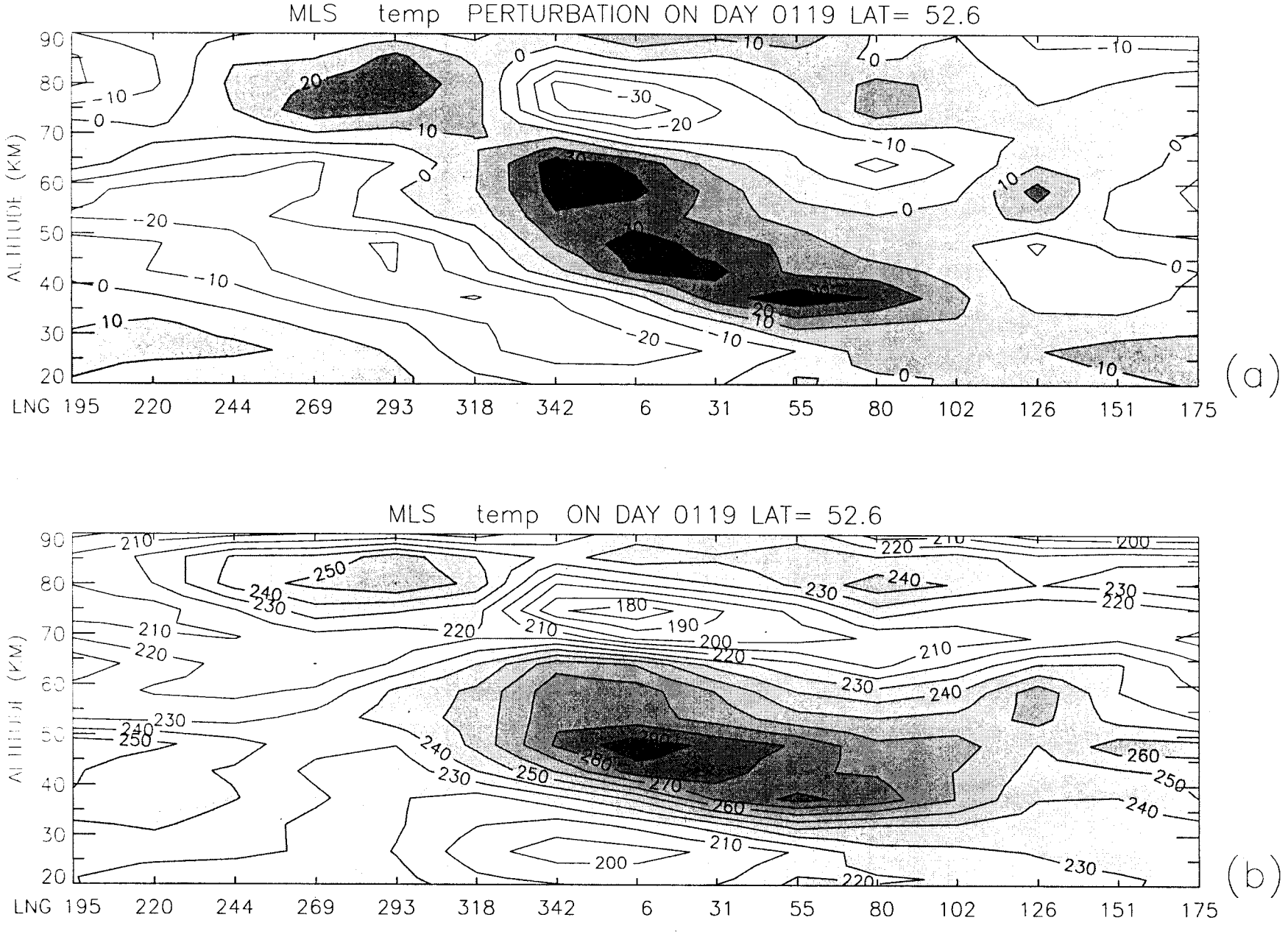
MLS temp PERTURBATION ON DAY 0119 LAT= 52.6
ALTITUDE (KM)
90
80
70
60
50
40
30
20
LNG 195 220 244 269 293 318 342 6 31 55 80 102 126 151 175
(a)
MLS temp ON DAY 0119 LAT= 52.6
ALTITUDE (KM)
90
80
70
60
50
40
30
20
LNG 195 220 244 269 293 318 342 6 31 55 80 102 126 151 175
(b)

Figure 2.

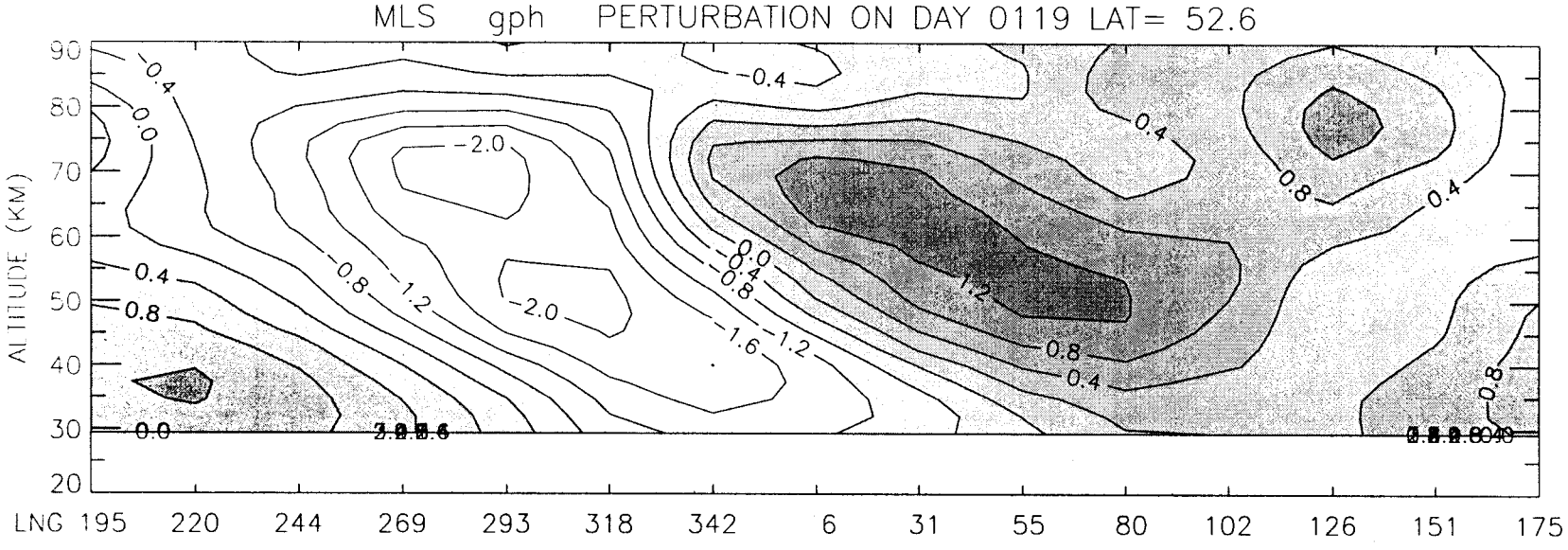
MLS gph PERTURBATION ON DAY 0119 LAT= 52.6
ALTITUDE (KM)
90
80
70
60
50
40
30
20
LNG 195 220 244 269 293 318 342 6 31 55 80 102 126 151 175
-0.4
0.0
-2.0
-0.8
-1.2
0.4
0.8
-1.6
1.2

Figure 3.

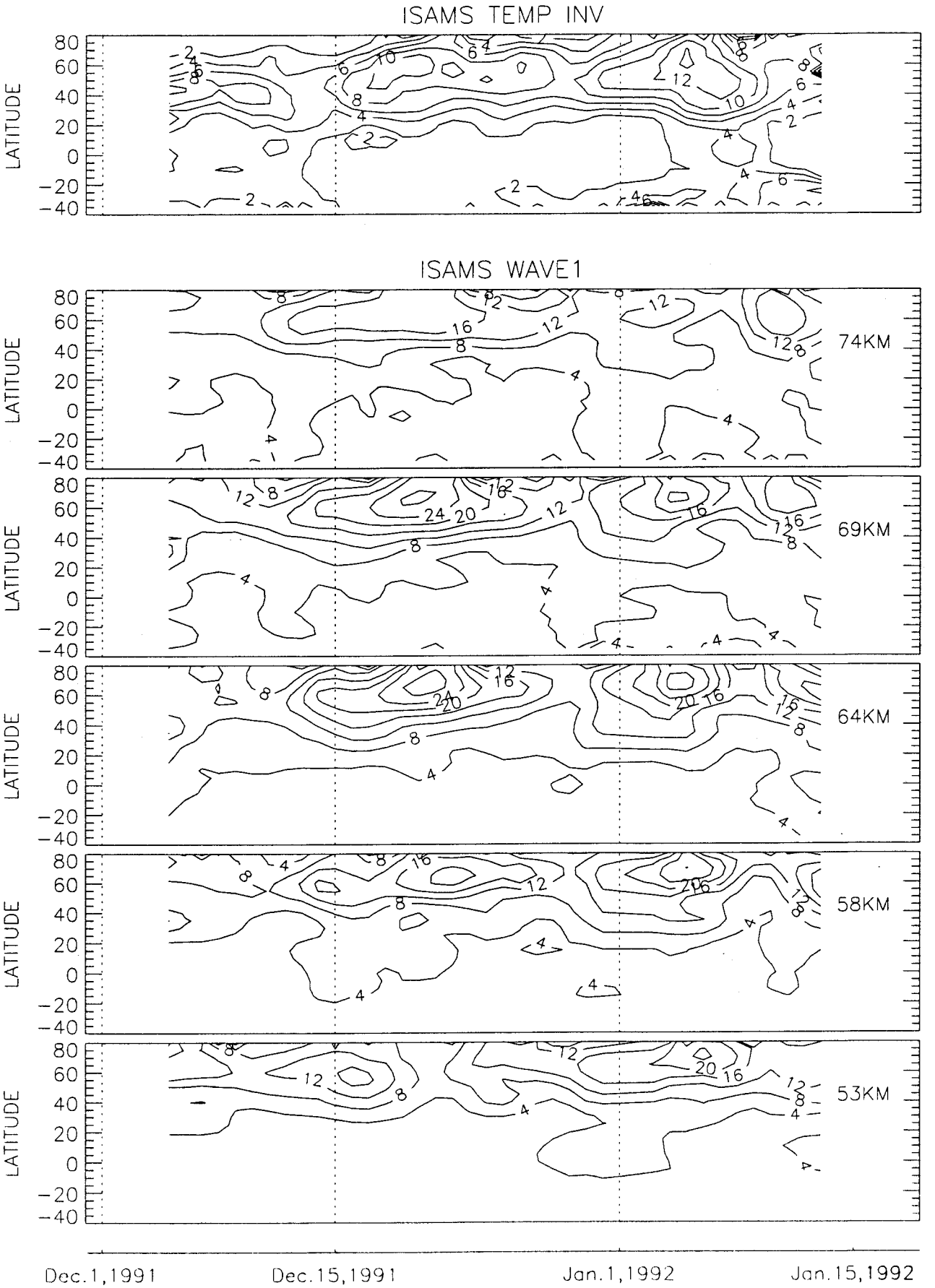
ISAMS TEMP INV
ISAMS WAVE1
LATITUDE
80
60
40
20
0
-20
-40
74KM
69KM
64KM
58KM
53KM
Dec.1,1991
Dec.15,1991
Jan.1,1992
Jan.15,1992

Figure 4.

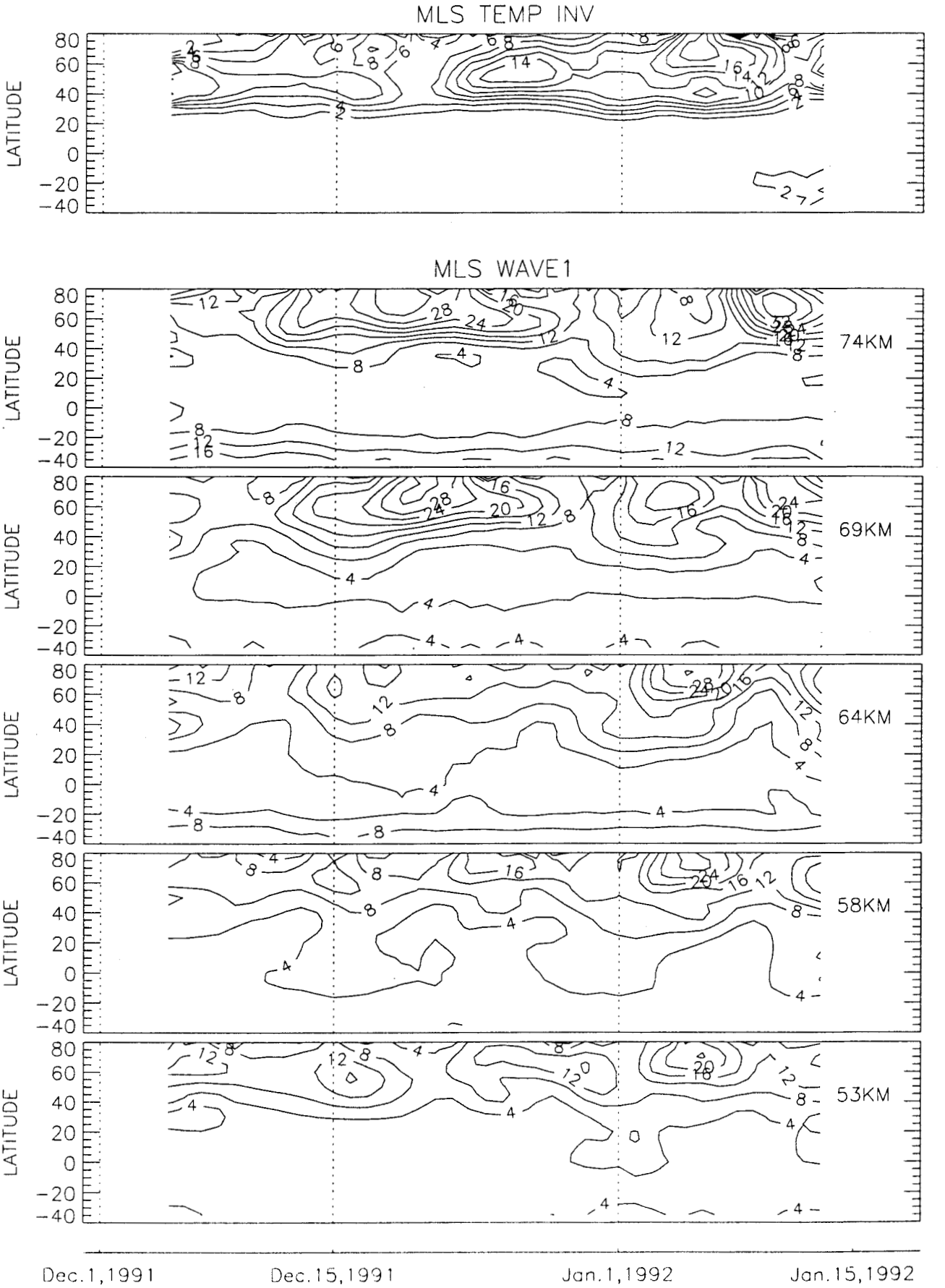
MLS TEMP INV
MLS WAVE1
LATITUDE
80
60
40
20
0
-20
-40
74KM
69KM
64KM
58KM
53KM
Dec.1,1991
Dec.15,1991
Jan.1,1992
Jan.15,1992

Figure 5.

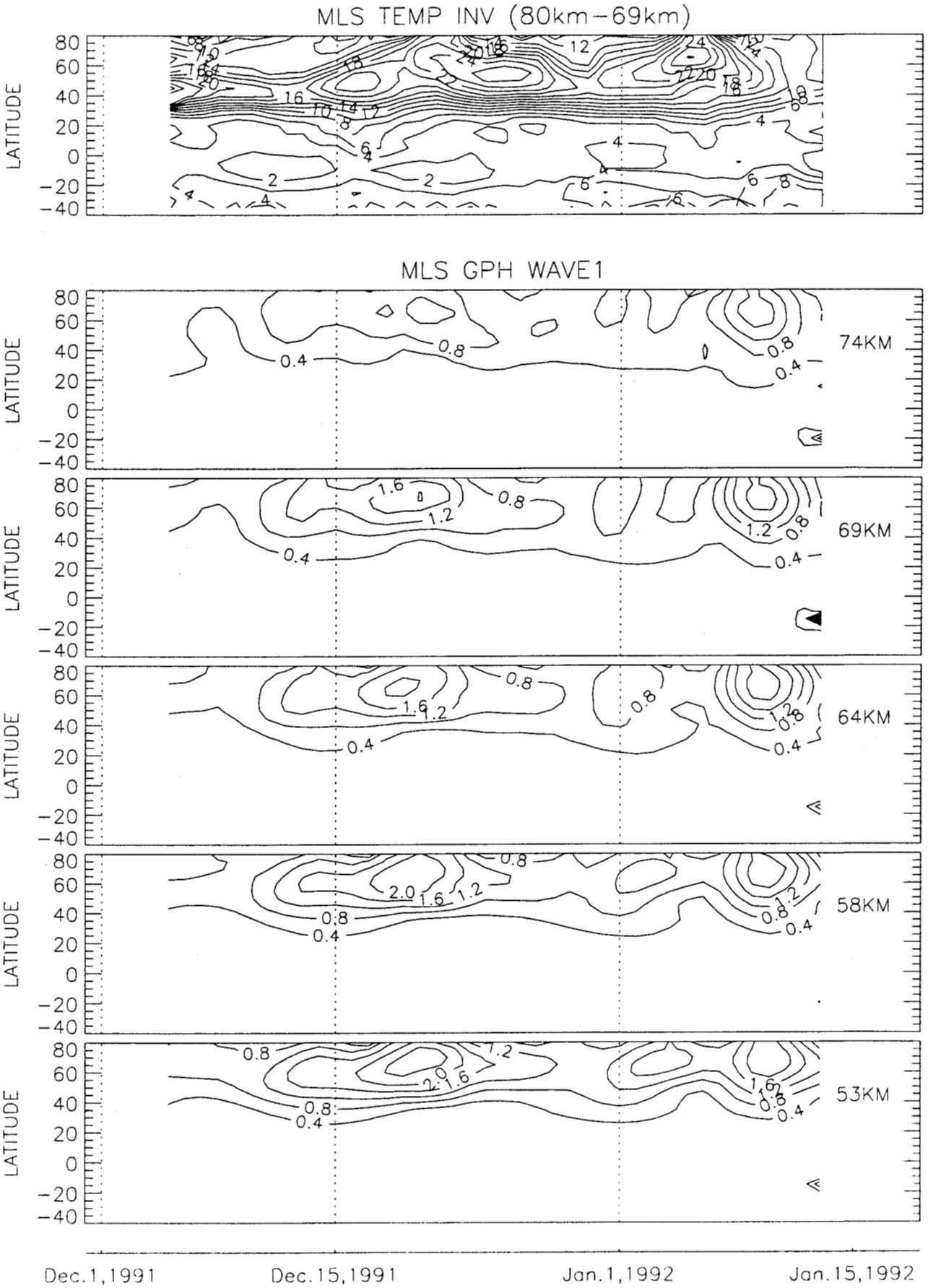
MLS TEMP INV (80km−69km)
MLS GPH WAVE1
74KM
69KM
64KM
58KM
53KM
LATITUDE
80
60
40
20
0
−20
−40
Dec.1,1991
Dec.15,1991
Jan.1,1992
Jan.15,1992

Figure 6.

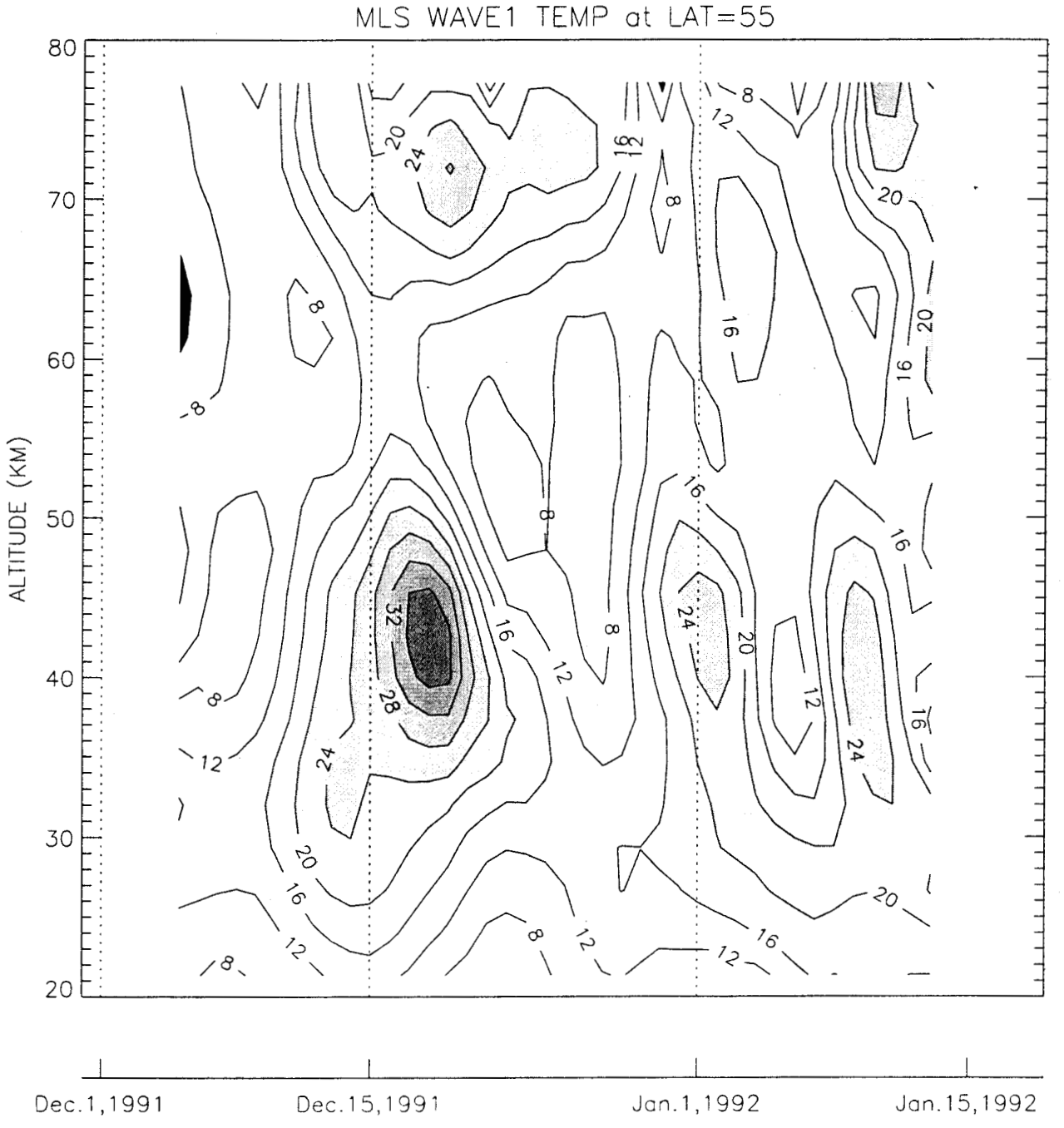
MLS WAVE1 TEMP at LAT=55
ALTITUDE (KM)
80
70
60
50
40
30
20
Dec.1,1991
Dec.15,1991
Jan.1,1992
Jan.15,1992

Figure 7.

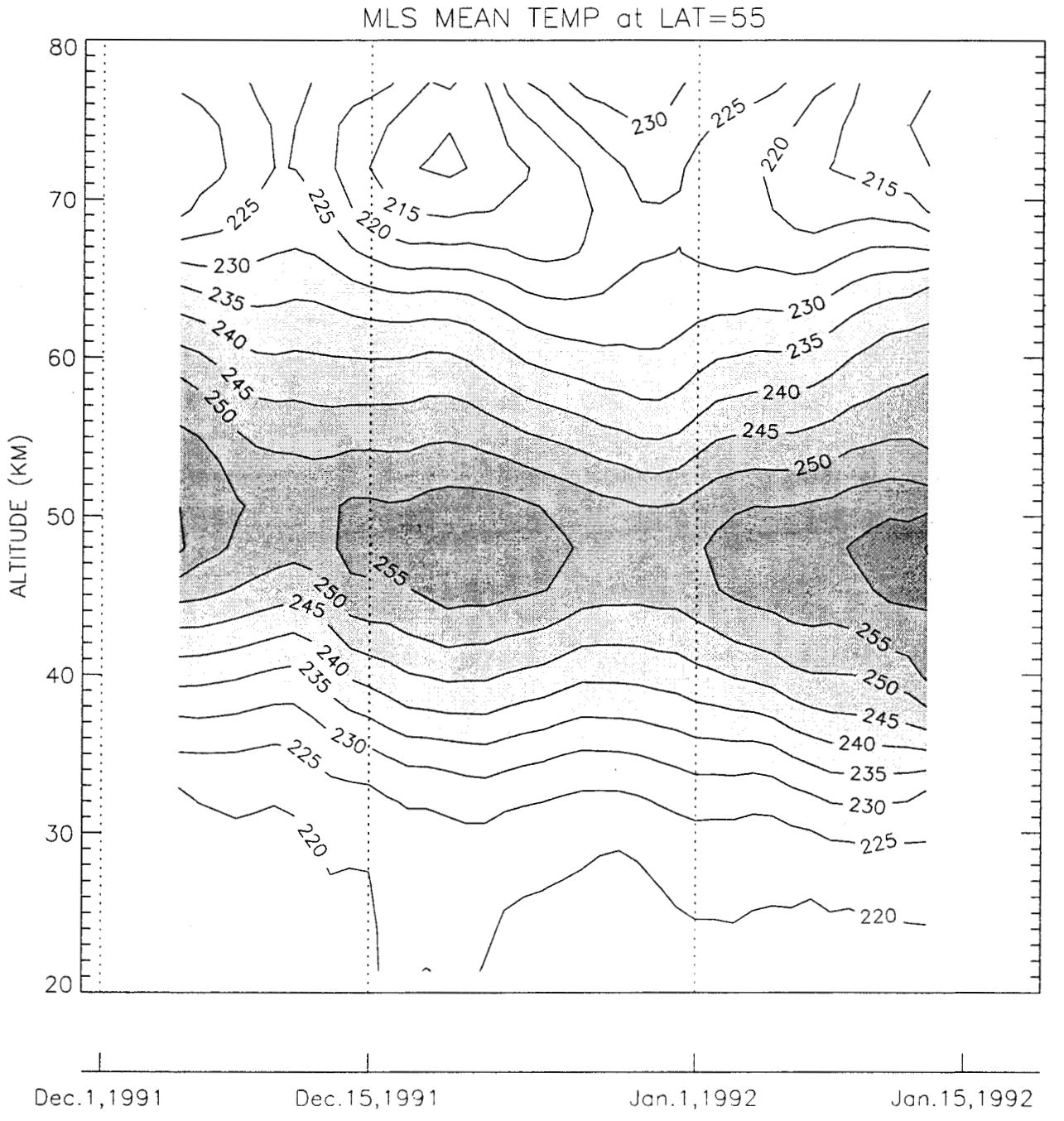
MLS MEAN TEMP at LAT=55
ALTITUDE (KM)
80
70
60
50
40
30
20
Dec.1,1991
Dec.15,1991
Jan.1,1992
Jan.15,1992
225
230
215
220
235
240
245
250
255

Figure 8.

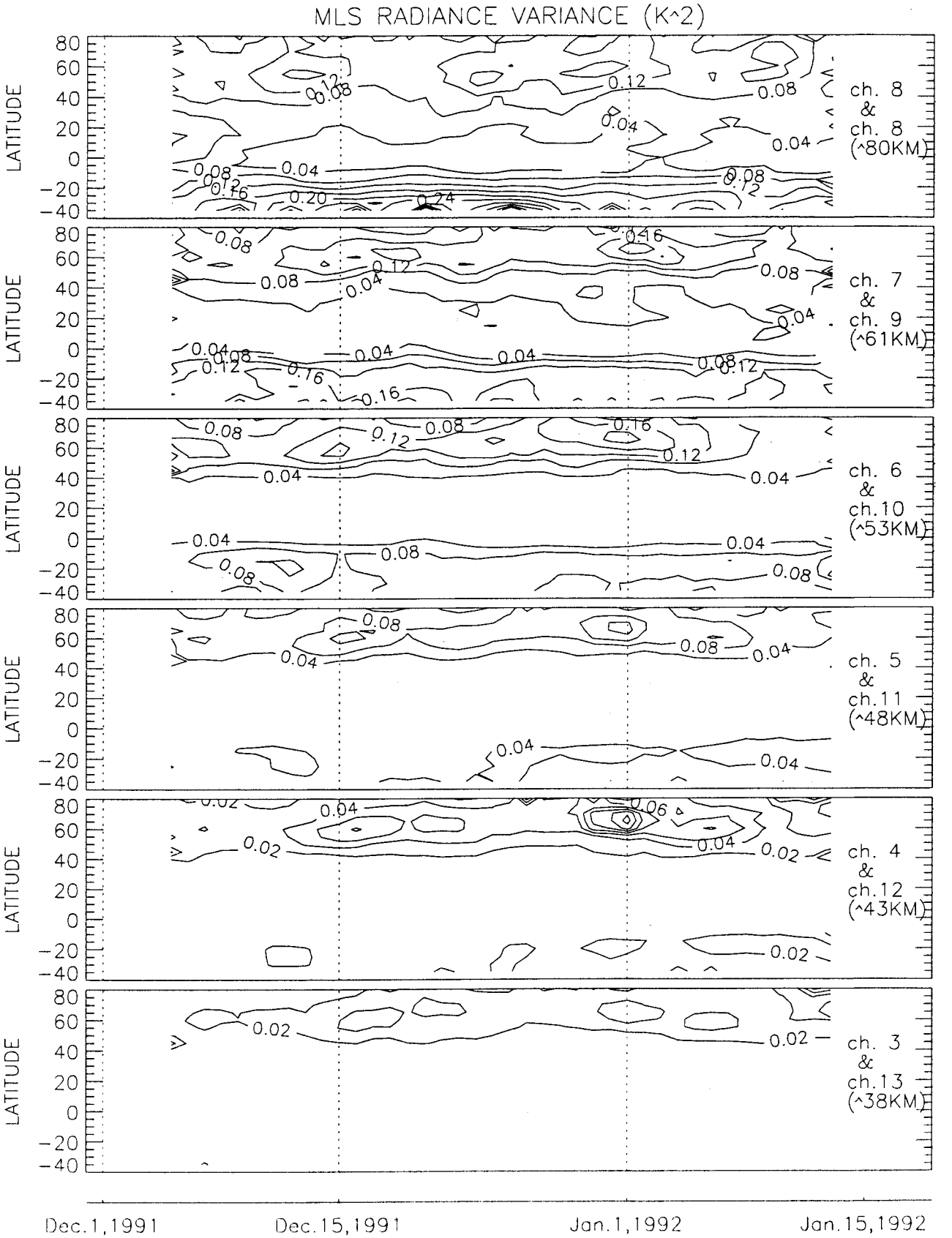
MLS RADIANCE VARIANCE (K^2)
LATITUDE
80
60
40
20
0
-20
-40
ch. 8
&
ch. 8
(^80KM)
ch. 7
&
ch. 9
(^61KM)
ch. 6
&
ch.10
(^53KM)
ch. 5
&
ch.11
(^48KM)
ch. 4
&
ch.12
(^43KM)
ch. 3
&
ch.13
(^38KM)
Dec.1,1991
Dec.15,1991
Jan.1,1992
Jan.15,1992

Figure 9.